Received: 12 February 2024 | Revised: 20 April 2024 | Accepted: 26 April 2024

DOI: 10.1111/ceo.14387

ORIGINAL ARTICLE - CLINICAL SCIENCE

Clinical & Experimental Ophthalmology WILEY

Evaluating keratometry and corneal astigmatism data from biometers and anterior segment tomographers and mapping to reconstructed corneal astigmatism

Achim Langenbucher PhD[1] | **Leonardo Taroni MD, PhD**[2] | **Catarina P. Coutinho MSc**[3] | **Alan Cayless PhD**[4] | **Nóra Szentmáry MD, PhD**[5] | **Peter Hoffmann MD**[6] | **Jascha Wendelstein MD**[1,7] | **Giacomo Savini MD, PhD**[8]

[1]Department of Experimental Ophthalmology, Saarland University, Homburg, Germany

[2]Department of Ophthalmology, Morgagni-Pierantoni Hospital, Forlì, Italy

[3]Ophthalmology, Studio Oculistico d'Azeglio, Bologna, Italy

[4]School of Physical Sciences, The Open University, Milton Keynes, UK

[5]Dr. Rolf M. Schwiete Center for Limbal Stem Cell and Aniridia Research, Saarland University, Homburg, Germany

[6]Augenklinik, Augen- und Laserklinik Castrop-Rauxel, Castrop-Rauxel, Germany

[7]Department of Ophthalmology, Johannes Kepler University Linz, Austria

[8]Ophthalmology, IRCCS Bietti Foundation, Rome, Italy

Correspondence
Achim Langenbucher, Department of Experimental Ophthalmology, Saarland University, Kirrberger Str 100 Bldg. 22, 66424 Homburg, Germany.
Email: achim.langenbucher@uni-saarland.de

Funding information
Fondazione Roma and the Ministero Italiano della Salute

Abstract

Background: To compare results from different corneal astigmatism measurement instruments; to reconstruct corneal astigmatism from the postimplantation spectacle refraction and toric intraocular lens (IOL) power; and to derive models for mapping measured corneal astigmatism to reconstructed corneal astigmatism.

Methods: Retrospective single centre study involving 150 eyes treated with a toric IOL (Alcon SN6AT, DFT or TFNT). Measurements included IOLMaster 700 keratometry (IOLMK) and total keratometry (IOLMTK), Pentacam keratometry (PK) and total corneal refractive power in 3 and 4 mm zones (PTCRP3 and PTCRP4), and Aladdin keratometry (AK). Regression-based models mapping the measured C0 and C45 components (Alpin's method) to reconstructed corneal astigmatism were derived.

Results: Mean C0 components were 0.50/0.59/0.51 dioptres (D) for IOLMK/PK/AK; 0.2/0.26/0.31 D for IOLMTK/PTCRP3/PTCRP4; and 0.26 D for reconstructed corneal astigmatism. All corresponding C45 components ranged around 0. The prediction models had main diagonal elements lower than 1 with some crosstalk between C0 and C45 (nonzero off-diagonal elements). Root-mean-squared residuals were 0.44/0.45/0.48/0.51/0.50/0.47 D for IOLMK/IOLMTK/PK/PTCRP3/PTCRP4/AK.

Conclusions: Results from the different modalities are not consistent. On average IOLMTK/PTCRP3/PTCRP4 match reconstructed corneal astigmatism, whereas IOLMK/PK/AK show systematic C0 offsets of around 0.25 D. IOLMTK/PTCRP3/PTCRP4. Prediction models can reduce but not fully eliminate residual astigmatism after toric IOL implantation.

KEYWORDS
corneal astigmatism, keratometry, posterior cornea measurement, toric intraocular lenses, total corneal power

1 | INTRODUCTION

Most optical biometers currently on the market provide keratometric measures in mm radius of curvature or dioptric power derived from corneal curvature data in a ring-shaped zone of diameter 2.0–3.6 mm. Where data are provided in dioptres (D) the measured radius of curvature is converted to dioptric power based on a keratometer index (n_K). If a standard keratometer setting is used when measuring the curvature, the exact measurement location depends on the curvature itself, with the result that for a flat cornea the measurement is taken more peripherally than with a steep cornea.

There is, however, no consensus in the literature as to a standard measurement protocol for toric intraocular lens (IOL) calculation. Options currently employed include: use of the anterior corneal surface keratometry only; application of a statistical nomogram[1–3] to approximate the mean corneal posterior surface astigmatism; and corneal tomography, which measures both corneal surfaces.

Each of the instruments currently in use has its own measurement protocol and produces differing sets of output data. For example, the IOLMaster 500 (Carl-Zeiss-Meditec, Germany) measures 6 points on the cornea at three meridians on a diameter of around 2.5 mm, whereas the IOLMaster 700 measures 18 points in total at three different radial zones of diameters from 1.5 to 3.3 mm. Other modern optical biometers provide total corneal power values representing a thin lens model of the cornea equivalent to the thick lens with separate anterior and posterior surfaces. However, even the total corneal power values are not standardised, with some instruments measuring within a central 3 or 4 mm zone, and others in a specific ring-shaped zone.

The current study aims to explore a unified strategy for reconstructing corneal astigmatism based on any of these varied approaches.

Since Javal's rule was first presented in 1890,[4] it is known that classical keratometry does not properly represent the astigmatism of the eye. In with-the-rule astigmatism of the cornea (WTR, steep corneal meridian between 60 degrees and 120 degrees)/against-the-rule (ATR, steep corneal meridian between 0 degrees and 30 degrees and between 150 degrees and 180 degrees) the astigmatism of the eye is overestimated/underestimated by around 0.5 dioptre. This means that if toric IOL calculation is based on keratometry without considering the posterior corneal surface astigmatism this will result in some ATR astigmatism after cataract surgery.

The literature contains many concepts for correcting keratometry for toric IOL calculation based on regressions[2,5–9] or nomograms[1,10] and artificial intelligence, but all of them depend systematically on the instrument and the correction strategy. The simplest approach involves mapping the preoperative keratometry to the preoperative total corneal power considering the effect of corneal posterior surface astigmatism only. Alternatively, mapping of the postoperative total corneal power additionally takes into account surgically induced changes in corneal astigmatism. Finally, the approach taken in this study of mapping the postoperative refraction would automatically include the effects of misalignment of optical elements in the eye, mainly IOL decentration and tilt, without having to measure these misalignments explicitly.

If a reliable spherocylindrical spectacle refraction after cataract surgery is known, together with the labelled power and orientation of the toric IOL measured at the slitlamp in the postoperative follow-up examination, the astigmatism of the corneal spherocylindrical power at the corneal plane can be reconstructed using backward vergence transformation (reconstructed corneal astigmatism).

This reconstructed value is based on the refractive cylinder of the spectacle refraction and the toric IOL toricity at the lens plane. If these are reliably recorded, the reconstruction automatically accounts for the systematic component of the posterior corneal astigmatism as well as changes in corneal astigmatism caused by the corneal incision and any misalignment of the toric IOL.

The purposes of the present study were

- to investigate the differences of keratometric and total corneal astigmatism values derived from a number of optical biometers and corneal anterior segment tomographers commonly used for toric IOL calculation,
- to reconstruct the corneal astigmatism value from the power and orientation of the toric IOL and the spherocylindrical refraction after cataract surgery, and
- to develop a multivariate regression model to map the astigmatic vector components of keratometric or total corneal astigmatism to the respective vector components of the reconstructed corneal astigmatism.

2 | METHODS

2.1 | Dataset for our study and surgical details

A dataset with $N = 150$ clinical data entries (from $N = 150$ patients) from the IRCCS Bietti Foundation (Rome, Italy) was considered for this retrospective study. All data were anonymized at source and stored in a .XLSX file, which was transferred to the Department of Experimental Ophthalmology for further analysis. Data tables were reduced to the relevant parameters required for our analysis, consisting of patient age in years, gender and laterality of the eye (OS or OD), and the corresponding measurement parameters as reported by each device/measurement modality in the study as listed below, together with the specifications of the toric IOL implanted in each case.

2.1.1 | IOLMaster 700 (Carl-Zeiss-Meditec, Jena, Germany)

Axial length (AL) in mm, anterior chamber depth (ACD) in mm (considered from the corneal epithelium to the front apex of the crystalline lens), central thickness of the crystalline lens (LT) in mm, horizontal corneal diameter (CD) in mm, keratometry in the flat meridian (IOLMKF in dioptres) and in the steep meridian [IOLMKS in dioptres at IOLMKA in degrees (°)], and total keratometry in the flat meridian (IOLMTKF in dioptres) and in the steep meridian (IOLMTKS in dioptres at IOLMTKA in degrees).

2.1.2 | Pentacam AXL (Oculus, Wetzlar, Germany)

Keratometry in the flat meridian (PKF in dioptres) and in the steep meridian (PKS in dioptres at PKA in degrees), astigmatism of total corneal refractive power in the 3 mm zone and centred on the pupil (PTCRP3 in dioptres at the steep axis PTCRP3A in degrees), and astigmatism of total corneal refractive power in the 4 mm zone and centred on the pupil (PTCRP4 in dioptres at the steep axis PTCRP4A in degrees).

2.1.3 | Aladdin (Topcon, Tokyo, Japan)

Keratometry in the flat meridian (AKF in dioptres) and in the steep meridian (AKS in dioptres at AKA in degrees).

2.1.4 | Manual refraction

Sphere (REFS in dioptres, derived in steps of 0.25 dioptres) and cylinder (REFC in dioptres, derived in steps of 0.25 dioptres at REFA in degrees) measured by the surgeon of the study (GS) at a refraction lane distance of 4 m at the postoperative follow-up examination. In the final step of manual refraction, confirmation that full distance correction had been achieved was obtained by noting that addition of a further +0.25 D of correction resulted in a reduction of visual acuity.

2.1.5 | Toric intraocular lens

Toric IOL model either SN6AT (IQ toric, $N = 107$), TFNT (Panoptix toric, $N = 16$) or DFT (Vivity toric, $N = 27$) (all Alcon, Fort Worth, USA), spherical equivalent power (IOLSE in dioptres) and toric power of the lens [IOLT in dioptres implanted at IOLA in degrees as measured at the slit lamp at the postoperative follow-up examination indicating the (marked) flat axis of the toric IOL].

Eyes with missing or incomplete data in any of the above-mentioned values were excluded at the source. All eyes were measured before cataract surgery with the IOLMaster, Pentacam AXL, Aladdin and 4–6 weeks postoperatively with manual refraction and slit lamp images to evaluate IOLA.

All surgeries were performed between January 2019 and November 2023 by an experienced surgeon (GS) under topical anaesthesia. After para-limbal 2.4 mm micro incision from the temporal side the anterior chamber was filled with a cohesive OVD, and a continuous curvilinear capsulorhexis (CCI) slightly smaller than the IOL optic diameter (approximately 5.25 mm) was created. After a standard phacoemulsification procedure, the toric IOL was inserted and aligned with a reference marker based on the average of PTCRP3A and PTCRP4A, taking special care that all viscoelastic behind and surrounding the IOL was removed and the CCI and both paracenteses were hydrated. The Institutional Review Board provided a waiver for this study (Ärztekammer des Saarlandes, 157/21). Informed consent of the patients was not required. The study followed the tenets of the Declaration of Helsinki.

2.2 | Preprocessing of the data

The data were transferred to MATLAB (MATLAB 2022b, MathWorks, Natick, USA) for further processing. Custom software was written in MATLAB to decompose the keratometric data (IOLMaster 700 IOLMKF/IOLMKS/IOLMKA, Pentacam PKF/PKS/PKA, and Aladdin AKF/AKS/AKA),

total keratometry data (IOLMaster 700 IOLMTKF/IOLMTKS/IOLMTKA), TCRP astigmatism Pentacam AXL in the 3 mm zone PTCRP3/PTCRP3A and 4 mm zone (PTCRP4/PTCRP4A), toric IOL power data (labelled IOLEQ and IOLT and postoperatively measured IOLA), and refraction data (REFS/REFC/REFA) from standard notation into power vector components in terms of (spherical) equivalent power EQ (except for Pentacam TCRP in the 3 and 4 mm zone) and the astigmatism projected to the 0°/90° meridian C0, and astigmatism projected to the 45°/135° meridian C45.[11,12] The defocus equivalent DEQ was taken as an overall quality metric for refractive outcome after toric IOL implantation and was derived from the power vector components of spectacle refraction by $DEQ = \sqrt{REFEQ2 + \frac{1}{4} \cdot (REFC0^2 + REFC45^2)}$.

2.3 | Reconstruction of the astigmatism of corneal spherocylindrical power

For this calculation, we assume a simplified pseudophakic eye model having three refracting surfaces: a thin lens spectacle refraction at vertex distance (VD) = 12 mm in front of the cornea; a thin lens cornea; a thin lens model of a toric IOL at an effective lens position (ELP) behind the cornea, and with the focal plane at AL behind the cornea. The spectacle correction is separated from the cornea by air (with refractive index 1.0). The toric IOL is separated from the cornea by aqueous humour (with a refractive index $n_A = 1.336$[13]), and from the retina by vitreous humour (with a refractive index $n_V = 1.336$[14]). The ELP was derived according to the Haigis formula[15] based on a linear regression with an intercept a_0 and scaling a_1 for the ACD and a_2 for AL, and using the optimised formula constants as listed in IOLCon (https://IOLCon.org, accessed on 26 March 2024). For the SN6AT, we used $a_0/a_1/a_2 = -0.111/0.249/0.179$, for the TFNT −0.036/0.319/0.175, and for the DFT 1.476/0.233/0.122, respectively. For our calculation, we did not consider the effect of surgically induced astigmatism (SIA).

Assuming the retina to be at the focal plane, the vergence at the ELP plane was (AL-ELP)/n_V. The spherocylindrical vergence in front of the lens is derived considering the toric IOL in terms of its 3 power vector components (IOLEQ, IOLC0 and IOLC45). Back-tracing this vergence through the aqueous humour with a distance ELP yields the spherocylindrical vergence directly behind the corneal front surface plane.[9,16–18] We then assume a corrected optical system with zero vergence in front of the spectacle correction and calculate the spherocylindrical vergence directly behind the spectacle plane considering the power vector components of postoperative refraction (REFEQ, REFC0 and REFC45). Tracing this vergence through VD, we read out the spherocylindrical vergence directly in front of the corneal front surface plane. The power vector components of the cornea are then derived by subtracting the respective components (RCAEQ, RCAC0 and RCAC45) directly before and after the corneal front surface plane. The power vector components RCAC0 and RCAC45 indicating the reconstructed corneal astigmatism are then considered as a reference for comparison with the different measurement techniques of corneal power.

2.4 | Prediction models to map power vector components to reconstructed corneal astigmatism

To generate a bivariate linear prediction model to map the vector components of the measured corneal astigmatism to the reconstructed corneal astigmatism vector components we used maximum likelihood estimation with an iterative ECM algorithm.[14,19] This Expectation/Conditional Maximization algorithm estimates robust model parameters for multiple linear regression problems. The respective results are described in terms of LogL as the value of the log likelihood objective function after the final iteration and the root-mean-squared value of the L2 vector norm of the residuals as a measure for the prediction performance.[19] With the IOLMaster 700, MIOLMK describes the mapping of keratometry (IOLMKC0 and IOLMKC45) to reconstructed corneal astigmatism (RCAC0 and RCAC45) and MIOLMTK describes the mapping of total keratometry (IOLMTKC0 and IOLMTKC45) to reconstructed corneal astigmatism. With the Pentacam AXL, MPK describes the mapping of keratometry (PKC0 and PKC45) to reconstructed corneal astigmatism, and MPTCRP3/MPTCRP4 describe the mapping of total corneal refractive power (PTCRP3C0 and PTCRP3C45/PTCRP4C0 and PTCRP4C45) to reconstructed corneal astigmatism. With the Aladdin, MAK describes the mapping of keratometry (AKC0 and AKC45) to reconstructed corneal astigmatism.

2.5 | Statistical analysis and data presentation

Data are listed exploratively in terms of the arithmetic mean, standard deviation (SD), median, and the lower and upper boundaries of the 95% confidence interval (2.5% and 97.5% quantiles). Each eye was treated as a separate case, and we did not implement a statistical correction strategy where both eyes of an individual were

included in the analysis. The astigmatic power vector components C0 and C45 were analysed using double angle plots showing the C0/C45 vector component in the X/Y axis. Royston's test has been used to test the bivariate astigmatism/cylinder vector with the C0 and C45 component against a bivariate normal distribution.[20,21] This test is considered as a generalisation of the Shapiro–Wilk test for multivariate normality and involves a correction for the correlation between the vector components in the sample.[20] A significance level of $p < 0.05$ was considered statistically significant. As a simplification, assuming bivariate normal distributions for the astigmatic power vector components, error ellipses for the 95% confidence intervals were calculated from the variance–covariance matrices and the centroids.[22] The areas of the error ellipses (derived from the eigenvalues and eigenvectors) were documented together with the areas of the ellipses indicating the data scatter. In addition, the 95% confidence region was calculated without assumptions of parametric distributions by iteratively eroding the data clouds according to their convex hull envelope (iterative convex hull stripping),[22,23] and the areas of the 95% confidence region and the spatial median (medoid) were derived.[22,24,25]

3 | RESULTS

The mean age of the 137 (80 female and 57 male) patients was 72.95 ± 9.81 years (median 74 years). Sixty-six left eyes and 84 right eyes were included. According to Pentacam keratometry, 82/49/19 eyes showed a WTR/ATR/oblique (OBL) astigmatism. In Table 1, the most relevant explorative data for the $N = 150$ eyes are listed in terms of mean, standard deviation, median and the bounds of the 95% confidence interval for biometric measures AL, ACD, LT, WTW, for the power of the toric IOL IOLEQ and IOLT, and for the postoperative refraction REFEQ and REFC.

Table 2 shows the astigmatic power vector components C0 and C45 for the IOLMaster 700 keratometry and total keratometry, for the Pentacam keratometry and TCRP in the 3 and 4 mm zone, and for Aladdin keratometry together with the respective components of the reconstructed corneal astigmatism. It can be seen that the values for all keratometry measurements (IOLMKC0, PKC0 and AKC0) range around 0.5 dioptres, whereas the values for all measurements considering the surface power of the anterior and posterior cornea (IOLMTKC0, PTCRP3C0 and TCRP4C0) as well as those for the reconstructed corneal astigmatism component RCAC0, are systematically lower with a range around 0.25–0.3 D. However, the C45 components of all measurements range around 0.0 D.

The coordinates of the centroids together with the area of the error ellipses, the coordinates of the spatial medians together with the areas of the confidence regions, and the Royston statistics[20,21] are listed in Table 3 together with the significance level p for a test of the bivariate astigmatism vectors for normality.

From the graphs for the IOLMaster 700 (Figure 1, top row) and the data listed in Table 3, it can be seen that the centroids of the distributions for both keratometry and total keratometry are located closer to zero as compared to the spatial medians. This effect is less marked for the Pentacam and not present in the Aladdin results.

Due to the fact that none of the bivariate astigmatic power vectors follow a bivariate normal distribution the 95% confidence regions derived from iterative erosion do not exactly match the 95% error ellipses (Figure 2).

Table 4 lists the definition of the bivariate linear prediction models which transform the vector components C0 and C45 of corneal astigmatism measured with the IOLMaster 700, Pentacam AXL and Aladdin biometer to the respective vector components of corneal power reconstructed from the power and orientation of the toric IOL implant and spherocylindrical refraction after cataract surgery.

TABLE 1 Explorative listing of most relevant preoperative biometric measurements axial length AL, anterior chamber depth ACD (measured from the corneal epithelium to the front apex of the crystalline lens), and thickness of the crystalline lens LT, and horizontal corneal diameter CD as derived with the IOLMaster 700 (IOLM), equivalent and toric power of the implanted tIOL (IOLEQ and IOLT), and postoperative refraction (spherical equivalent REFEQ, cylinder REFC and defocus equivalent DEQ).

$N = 150$	AL in mm	ACD in mm	LT in mm	CD in mm	IOLEQ in D	IOLT in D	REFS in D	REFC in D	DEQ in D
Mean	24.085	3.003	4.478	11.786	21.271	1.908	−0.444	0.362	0.566
SD	1.667	0.454	0.454	0.439	4.748	1.123	0.874	0.409	0.846
Median	23.845	3.060	4.520	11.800	21.7504	1.500	0.000	0.250	0.354
2.5% quantile	21.305	2.215	3.533	10.809	9.438	1.000	−3.219	0.000	0.000
97.5% quantile	27.955	3.835	5.368	12.600	30.469	5.813	0.250	1.250	3.324

Note: Mean, SD, Median, 2.5%/97.5% quantile refer to the arithmetic mean, standard deviation, median and the lower and upper bounds of the 95% confidence interval respectively, and D refers to dioptre.

TABLE 2 Astigmatic vector components [projections to the 0°/90° meridian (C0) and to the 45°/135° meridian (C45)] for keratometry and total keratometry with the IOLMaster 700, keratometry and TCRP in a 3 and 4 mm zone with the Pentacam AXL, and keratometry with the Aladdin, together with the reconstructed corneal astigmatism as calculated from the spherocylindrical vergences directly in front of and behind the corneal front surface plane. Mean, SD, Median and 2.5%/97.5% quantile refer to the arithmetic mean, standard deviation, median and the lower and upper bounds of the 95% confidence interval, respectively.

$N = 150$, all data	IOLMaster 700				Pentacam AXL						Aladdin		Reconstructed corneal astigmatism	
	Keratometry		Total keratometry		Keratometry		TCRP 3 mm		TCRP 4 mm		Keratometry			
in dioptres	C0	C45	C0	C45	C0	C45	C0	C45	C0	C45	C0	C45	C0	C45
Component														
Mean	0.500	−0.021	0.248	−0.076	0.592	−0.017	0.261	−0.031	0.309	−0.027	0.509	0.020	0.258	0.030
SD	1.415	0.797	1.441	0.793	1.398	0.769	1.221	0.748	1.306	0.752	1.437	0.808	1.375	0.899
Median	0.816	−0.039	0.555	−0.073	0.646	−0.077	0.402	0.001	0.371	0.006	0.531	0.000	0.510	0.000
2.5% quantile	−1.787	−1.349	−2.188	−1.392	−1.772	−1.399	−1.871	−1.259	−1.959	−1.438	−1.763	−1.452	−2.350	−1.746
97.5% quantile	3.861	1.385	3.711	1.336	4.109	1.389	3.203	1.647	3.469	1.564	4.354	1.521	3.078	2.094

4 | DISCUSSION

It has been well known in ophthalmology for many decades that keratometry restricted to the corneal front surface only does not properly reflect the astigmatism of the entire eye. Even though Javal's rule published some 100 years ago[4] and the modifications shown by Grosvenor[26,27] could be used as a rule of thumb in clinical routine, these may oversimplify the real correlation between the astigmatism of the anterior and posterior corneal surface. Additionally, there are complimentary effects such as decentration and tilt of optical elements which could also affect the astigmatism of the eye. What our data on 150 eyes with implantation of a toric IOL clearly show, is that even modern tomographic measurement techniques which assess both corneal surfaces such as the Pentacam Scheimpflug tomographer (with the TCRP data in the 3 and 4 mm zone) or the IOLMaster 700 (with the total keratometry) do not exactly agree in their measurements of the total corneal power of a cornea. Measurement of the corneal front surface curvature, for example with a keratometer or a Placido, Scheimpflug or optical coherence tomographer is quite simple because we have direct access to this first refractive surface in the optical pathway.[28,29] However, for measuring deeper structures in the eye (even for the posterior corneal surface) the measured structure is no longer viewed directly and is subject to optical magnification. Just as the entrance pupil is a magnified image of the real pupil through the cornea, the posterior corneal surface as measured by a tomographer has to be corrected for the imaging properties of the cornea, for example using reverse raytracing.[9,17] Provided that the corneal front surface is described in terms of a simple refracting surface (e.g., a rotationally symmetric quadric surface) such an image correction is quite simple, and in some cases a simplification based on a homogeneous 'image magnification' might be sufficient. However, with arbitrary surface shape and especially with topographic irregularities, image distortions could have a significant impact, potentially making the reverse raytracing more complex. As a result, data processing in most of the tomographers may simplify this correction process for image distortion for example using a 2D reverse raytracing (separated for each meridian) instead of a 3D correction.

One of the largest challenges in modern cataract surgery with implantation of toric IOLs is the extraction of a representative value for the corneal astigmatism to be corrected with the toric IOL.[2,3,5,7,8,10,18,28–34] Several different approaches are available to surgeons, including direct use of keratometric measures, keratometric measures with a statistical correction for the posterior corneal astigmatism,[32] tomographic measures for the anterior

TABLE 3 Explorative listing of the X and Y coordinates for the centroid and the area of the 95% error ellipse, and the X and Y coordinates of the spatial median and the area of the 95% confidence area for the corneal astigmatism vector with the IOLMaster 700 (keratometry IOLMK and total keratometry IOLMTK), with the Pentacam AXL [keratometry PK and total corneal refractive power derived from the 3 mm and 4 mm zone (PTCRP3 and PTCRP4)], with the Aladdin (keratometry AK), the reconstructed corneal astigmatism, and the postoperative spectacle refraction (REF).

$N = 150$		IOLMK	IOLMTK	PK	PTCRP3	PTCRP4	AK	Reconstructed corneal astigmatism	REF
Centroid coordinates and 95% error ellipse area	X in D	0.500	0.248	0.592	0.261	0.309	0.509	0.258	−0.060
	Y in D	−0.021	−0.076	−0.017	−0.031	−0.027	0.020	0.030	−0.042
	Area in D^2	20.952	21.224	20.218	17.187	28.458	21.755	23.249	2.755
Spatial median coordinates and 95% confidence region area	X in D	0.758	0.610	0.644	0.356	0.397	0.490	0.221	0.000
	Y in D	−0.039	0.000	−0.088	−0.183	0.053	−0.014	−0.039	0.000
	Area in D^2	12.547	12.778	16.482	12.749	15.613	15.886	20.147	2.521
Royston's test for multivariate normality	Royston's statistics/ p value	33.5 5.3e-8	31.0 1.9e-7	36.7 1.09e-8	18.8 8.4e-5	25.1 3.6e-6	37.6 6.7e-9	36.4 1.2e-8	76.2 <1e-10

Note: D refers to dioptre. Using Royston's test (Royston's statistics and significance level p), it was proven that none of the bivariate astigmatism vectors followed a bivariate normal distribution ($p < 0.05$).

and posterior corneal surface which define a thick lens model with two crossed cylinders, or total corneal power values from the tomographer as a thin lens 'replacement' for the two surface cornea.[28,29] More or less all tomographers offer such total corneal power values (called total keratometry, total power, real power, total corneal refractive power, true power, etc.) which simplify the cornea from two surfaces and crossed cylinders to a single refractive surface, but there are no standards as to whether data from the paracentral area (such as in keratometry) or integral values over any central region should be used,[32,33] or whether the thin replacement lens is located at the corneal front vertex plane (front vertex power of the two surface cornea), the corneal back vertex plane (back vertex power of the two surface cornea) or the principal plane of the cornea (equivalent lens).[9,16–18]

Therefore, the aim of this study was to separate out the differences between the measurement modalities commonly used in clinical practice for planning toric IOL implantations, and to show a simple mapping to a reference astigmatism which is independent from any corneal measurement. This mapping could be used in clinical practice where measurement data from the posterior cornea are unavailable. Since our dataset contains reliable data on postoperative manual refraction and the power data of the toric IOL (in terms of equivalent and toric power) together with orientation of the toric lens marker axis in mydriasis in the postoperative slitlamp biomicroscope measurement, it was possible to use a simple vergence transformation strategy to reconstruct the corneal spherocylindrical power from the spectacle refraction and the biometric data together with the toric IOL power and orientation in terms of a vergence deficit (between the vergence before and behind the corneal front vertex plane[9]). This reconstructed corneal power could be used as reference by the clinicians. Since the design data of the toric IOL were not available and therefore the principal plane of the lens is unknown, we simplified the toric IOL as a thin lens model located at the ELP predicted from a classical lens power formula. For this purpose we decided to use the Haigis formula[15] as the keratometer index $n_K = 1.3315$ used for conversion of corneal radius of curvature to corneal power seems to represent the conditions of an average cornea properly, with the consequence that the ELP more or less matches the real position of the lens in the eye. The bivariate vector of the reconstructed corneal astigmatism was used as a reference, and all measurements from the IOLMaster 700 (keratometry and total keratometry), the Pentacam (keratometry and TCRP in the 3 and 4 mm zone) and the Aladdin (keratometry from a Placido disc topographer) were mapped to this reconstructed corneal astigmatism vector.

Our results indicate that the C0 components of keratometry (IOLMKC0, PKC0 and AKC0) are on average larger (0.50, 0.59 and 0.51 D) compared with the corresponding total corneal power values based on a measurement of both corneal surfaces (0.25 D for IOLMTKC0, 0.26 D for PTCRP3C0, and 0.31 D for PTCRP4C0), which are on average well represented by the reconstructed 0.26 D for the RCAC0. Comparing the mean C0 values for keratometry and the total corneal power values it is obvious that Javal's rule,[4] with or without Grosvenor's

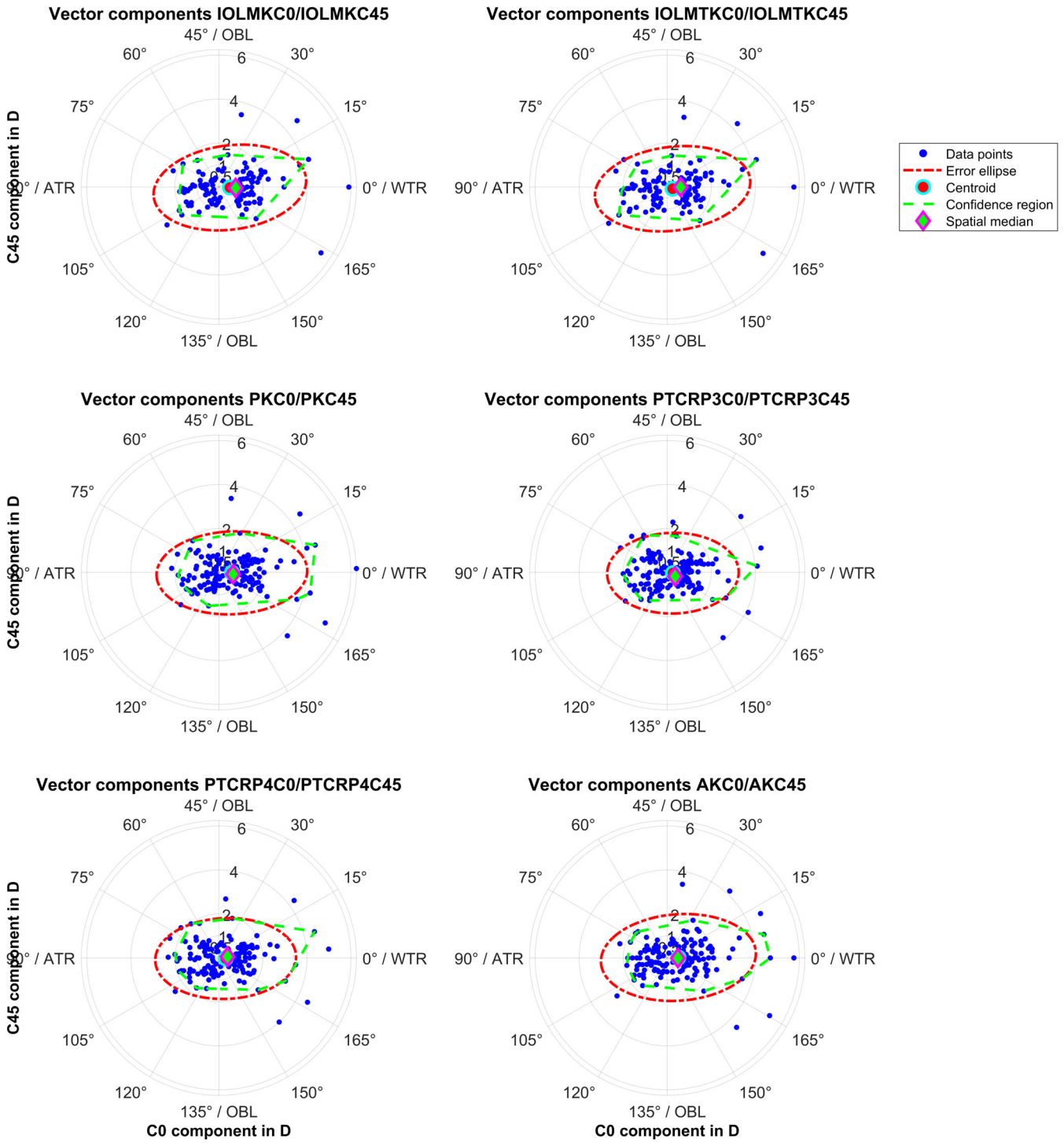

FIGURE 1 The double angle plot with the astigmatic power vector components (C0 and C45: projection to the 0/90° and to the 45°/135° meridian) for different measured modalities of corneal astigmatism using the IOLMaster 700, the Pentacam AXL and the Aladdin device.

modification,[25,26] indicates that the effect of the posterior corneal surface astigmatism may be much smaller in the real-life scenario (around 0.25 D against the rule) than 0.5 dioptres as recommended by Javal.[4]

However, it can also be seen from Figure 3 that even if the centroid or medoid of postoperative refraction is close to zero, that there is some variation in the residual refractive cylinder, and we cannot promise a full correction of the astigmatism with implantation of a toric IOL. Further, if we condense the refractive outcome after toric IOL implantation to the defocus equivalent DEQ as a single quality marker, we see that that this results in a

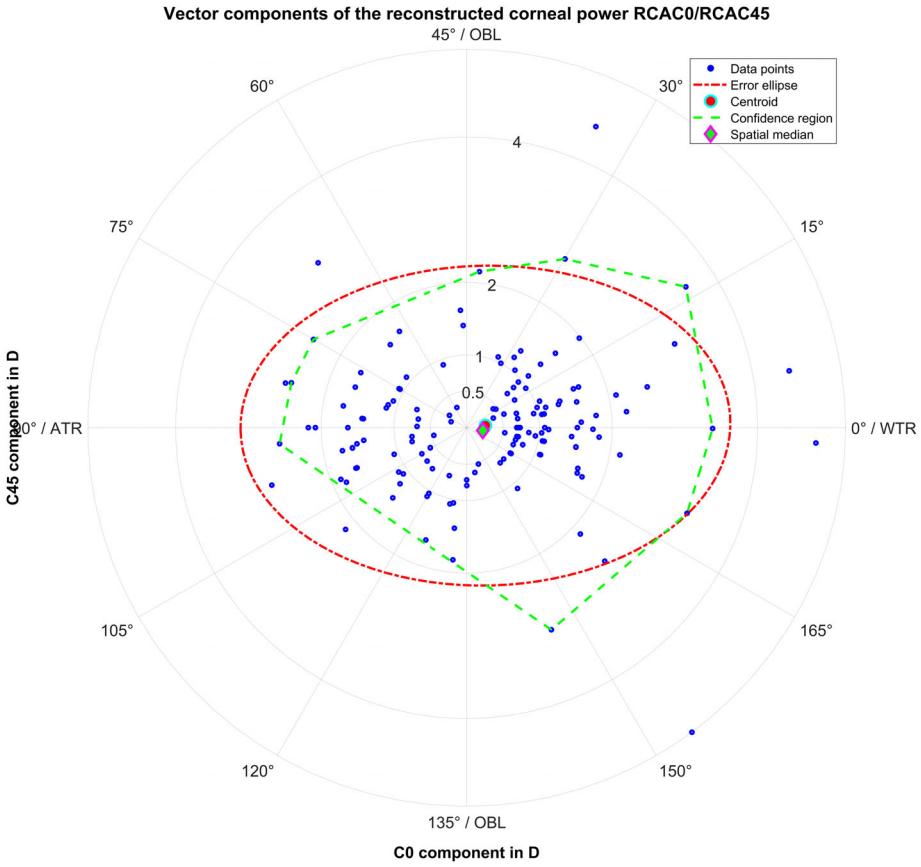

FIGURE 2 The double angle plot with the astigmatic power vector components for the reconstructed corneal astigmatism which is rated as the reference for the prediction models. Again, since the bivariate astigmatic power vector does not follow a bivariate normal distribution the 95% confidence region derived from iterative erosion does not exactly match the 95% error ellipse.

mean/median DEQ of 0.57/0.35 D. In part, this residual DEQ could be explained with the quantisation of power steps in the equivalent and cylinder power of the IOL and some quantisation in the postoperative refraction.

It was surprising to us that none of the bivariate astigmatism vectors follow a bivariate normal distribution. We also double-checked the statistics shown in Table 3 using the Henze-Zirkler test for multivariate normality (data not shown in this paper[20]). For evaluating astigmatic power vectors, this means that parametric statistical comparisons (e.g., with the Hotelling-T2 test) or data presentation (e.g., with 95% error ellipses derived from variance–covariance matrices) as performed in some papers could be questionable, and a test for bivariate or multivariate normality seems obligatory for data interpretation. We therefore decided to provide both the well-established error ellipses with the centroids (as parametric evaluations) and the error regions with the spatial medians (as nonparametric evaluations).[22–25]

The models which map keratometry or total corneal power vector components to the respective components of the reconstructed corneal astigmatism are designed to give a regression-based prediction model for the reconstructed corneal astigmatism data. Since the reconstructed corneal astigmatism refers to the thin spherocylindrical lens that would be required at the corneal front vertex plane to match the postoperative spectacle refraction to the toric IOL (with its labelled power and its orientation derived at the slitlamp biomicroscope) it seems suitable as a reference. Under perfect conditions (if corneal power measurements match to reconstructed corneal astigmatism), we would assume that the 2×2 matrices all are unit matrices with 1 at the main diagonal and 0 elsewhere, and for the 2×1 intercept vectors we would assume that for the total corneal power data (IOLMaster total keratometry and Pentacam TCRP in the 3 and 4 mm zone) is the 0 vector, and for the keratometry data (IOLMaster keratometry, Pentacam keratometry and Aladdin keratometry) we have some 'offset' in the first element (e.g., −0.25 D as the mean difference between C0 for total corneal power and keratometry based measures). However, our prediction models indicate that we consistently have main diagonal elements in the 2×2 matrices lower than 1 and some crosstalk between C0 and C45 components (i.e., some non-zero off-diagonal elements). As a consequence, the intercept vectors do not match to the mean differences between the reconstructed corneal astigmatism and the corneal power measurements (e.g., we get $[-0.138\ 0.097]^T$ MIOLMK instead of the mean differences $[-0.242\ 0.051]^T$).

However, our study has some limitations: firstly, our dataset includes data derived using 3 different models of

TABLE 4 Definitions of the bivariate prediction models for mapping the vector components C0 and C45 of keratometric astigmatism MIOLMK and total keratometry MIOLMTK of the IOLMaster 700, keratometric astigmatism MPK and total corneal refractive power in the 3 mm MPTCRP3 and 4 mm zone MPTCRP4 of the Pentacam AXL, keratometric astigmatism of the Aladdin MAK [all data in dioptres (D)] to the respective vector components of reconstructed corneal astigmatism (both data in D). logL refers to the log likelihood objective function at the last iteration, and L2 error to the root-mean-squared value of the residual L2 vector norm of mean residuum error.

Prediction model	Equation of the bivariate linear prediction model	logL	L2 error in D
MIOLMK	$\begin{bmatrix} BCAC0 \\ BCAC45 \end{bmatrix}_{predicted} = \begin{bmatrix} 0.798 & 0.086 \\ -0.131 & 0.739 \end{bmatrix} \cdot \begin{bmatrix} IOLMKC0 \\ IOLMKC45 \end{bmatrix} + \begin{bmatrix} -0.138 \\ 0.097 \end{bmatrix}$	−227	0.441
MIOLMTK	$\begin{bmatrix} BCAC0 \\ BCAC45 \end{bmatrix}_{predicted} = \begin{bmatrix} 0.779 & 0.069 \\ -0.125 & 0.724 \end{bmatrix} \cdot \begin{bmatrix} IOLMTKC0 \\ IOLMTKC45 \end{bmatrix} + \begin{bmatrix} 0.074 \\ 0.102 \end{bmatrix}$	−232	0.451
MPK	$\begin{bmatrix} BCAC0 \\ BCAC45 \end{bmatrix}_{predicted} = \begin{bmatrix} 0.979 & 0.129 \\ -0.074 & 0.567 \end{bmatrix} \cdot \begin{bmatrix} PTCRP3C0 \\ PTCRP3C45 \end{bmatrix} + \begin{bmatrix} 0.007 \\ 0.067 \end{bmatrix}$	−327	0.515
MPTCRP3	$\begin{bmatrix} BCAC0 \\ BCAC45 \end{bmatrix}_{predicted} = \begin{bmatrix} 0.979 & 0.129 \\ -0.074 & 0.567 \end{bmatrix} \cdot \begin{bmatrix} PTCRP3C0 \\ PTCRP3C45 \end{bmatrix} + \begin{bmatrix} 0.007 \\ 0.067 \end{bmatrix}$	−327	0.515
MPTCRP4	$\begin{bmatrix} BCAC0 \\ BCAC45 \end{bmatrix}_{predicted} = \begin{bmatrix} 0.933 & 0.103 \\ -0.080 & 0.579 \end{bmatrix} \cdot \begin{bmatrix} PTCRP4C0 \\ PTCRP4C45 \end{bmatrix} + \begin{bmatrix} -0.028 \\ 0.070 \end{bmatrix}$	−314	0.499
MKA	$\begin{bmatrix} BCAC0 \\ BCAC45 \end{bmatrix}_{predicted} = \begin{bmatrix} 0.844 & 0.161 \\ -0.091 & 0.670 \end{bmatrix} \cdot \begin{bmatrix} AKC0 \\ AKC45 \end{bmatrix} + \begin{bmatrix} -0.168 \\ 0.061 \end{bmatrix}$	−300	0.472

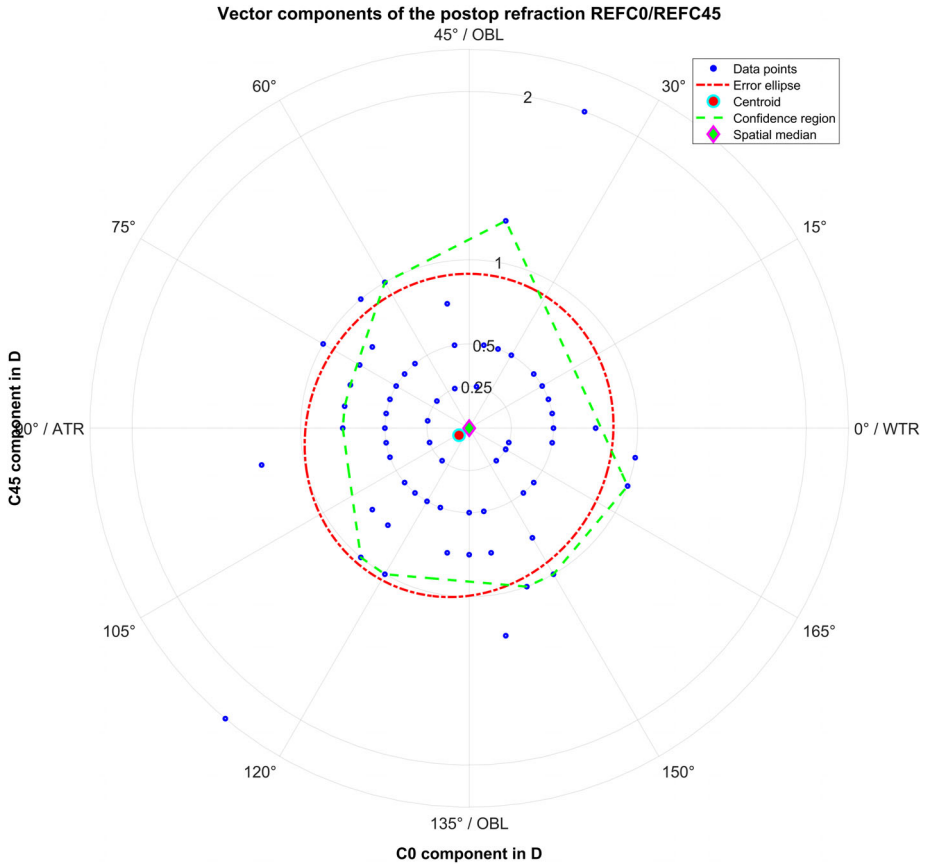

FIGURE 3 The double angle plot with the astigmatic power vector components REFC0 and REFC45 for the postoperative refraction. This graph shows that the bivariate distribution is well centred with both the centroid and spatial median close to zero, indicating that there is no systematic offset. However, we also see from the data scatter and the 95% error ellipse and the 95% error region that the astigmatism of the residual refraction after toric IOL implantation is not satisfactory and this suggests that better prediction models are required.

toric lens. However, since all of them are made by the same manufacturer from hydrophobic material and we used the respective optimised formula constants derived from IOLCon we feel it appropriate to consider the data as one study population. Second, as the reference for our prediction models we used the reconstructed corneal astigmatism vector which was back-calculated from the spectacle refraction and the labelled power and measured

orientation as a measure independent from any corneal tomographic measurement. However, we are aware that the reconstructed corneal astigmatism could also include some labelling error of the toric IOL, astigmatism due to lens tilt and decentration, or SIA which was not considered in this analysis (as we feel that the stochastic component of the SIA dominated the deterministic effect). And thirdly, in contrast to error ellipses and centroids used for bivariate vectors with normality, there is no unique concept for calculating the median or confidence region in case of non-normality.[22,24,25] However, from the literature we feel that iterative erosion is a proper way to extract the confidence region and the spatial median of a non-uniform bivariate distribution, which follows a strategy similar to the univariate case of deriving confidence intervals or the median.[23]

In conclusion, our results indicate that the differences between the centroids/medoids of classical keratometry based on corneal front surface data and total corneal power values based on tomographic data are on average in a range of 0.25 D for the C0 and 0.0 D for the C45 astigmatism vector component, much less than expected. Even if the centroid/medoid of the postoperative refractive cylinder is close to zero indicating no systematic residual refractive cylinder after toric IOL implantation, there is a large variation in the results and this implies that full astigmatism correction may not be achieved for all patients following toric IOL implantation. Linear bivariate regression-based prediction models could be used to map different measurement modalities of corneal astigmatism to the reference, which is extracted from a reconstruction using postoperative manual spectacle refraction and the labelled power and measured orientation of the toric lens. Larger studies with multicentric data are required to verify whether this reconstructed corneal astigmatism could qualify as reference.

ACKNOWLEDGEMENT

Open Access funding enabled and organized by Projekt DEAL.

FUNDING INFORMATION

The contribution of IRCCS Bietti Foundation was supported by Fondazione Roma and the Ministero Italiano della Salute.

CONFLICT OF INTEREST STATEMENT

Dr. Langenbucher reports speaker fees from Hoya Surgical and Johnson & Johnson Vision outside the submitted work. Ms. Coutinho reports speaker fees from Carl Zeiss Meditec AG. Dr. Cayless, Dr. Szentmáry and Dr. Taroni report no financial or proprietary interests. Dr. Hoffmann reports speaker fees from Hoya Surgical and Johnson & Johnson outside the submitted work. Dr. Wendelstein reports research grants from Carl Zeiss Meditec AG, speaker fees from Carl Zeiss Meditec AG, Alcon, Rayner, Bausch and Lomb and Johnson & Johnson Vision outside of the submitted work. Dr. Savini reports speaker fees from Alcon, Carl Zeiss Meditec AG, Johnson & Johnson Vision and SIFI outside of the submitted work.

DATA AVAILABILITY STATEMENT

The data that support the findings of this study are openly available in Untitled Item at https://figshare.com/, reference number 10.6084/m9.figshare.25205159.

ORCID

Achim Langenbucher https://orcid.org/0000-0001-9175-6177

Jascha Wendelstein https://orcid.org/0000-0003-4145-2559

REFERENCES

1. Chen TS, LaHood BR, Esterman A, Goggin M. Accuracy of the Goggin nomogram for 0.50 D steps in toric IOL cylinder power calculation. *J Refract Surg*. 2022;38(5):298-303. doi:10.3928/1081597X-20220404-01
2. Koch DD, Wang L, Abulafia A, Holladay JT, Hill W. Rethinking the optimal methods for vector analysis of astigmatism. *J Cataract Refract Surg*. 2021;47(1):100-105. doi:10.1097/j.jcrs.0000000000000428
3. Park DY, Lim DH, Hwang S, Hyun J, Chung TY. Comparison of astigmatism prediction error taken with the Pentacam measurements, Baylor nomogram, and Barrett formula for toric intraocular lens implantation. *BMC Ophthalmol*. 2017;17(1):156. doi:10.1186/s12886-017-0550-z
4. Elliott M, Callender MG, Elliott DB. Accuracy of Javal's rule in the determination of spectacle astigmatism. *Optom Vis Sci*. 1994;71(1):23-26.
5. Koch DD, Ali SF, Weikert MP, Shirayama M, Jenkins R, Wang L. Contribution of posterior corneal astigmatism to total corneal astigmatism. *J Cataract Refract Surg*. 2012;38(12):2080-2087. doi:10.1016/j.jcrs.2012.08.036
6. Koch DD, Jenkins RB, Weikert MP, Yeu E, Wang L. Correcting astigmatism with toric intraocular lenses: effect of posterior corneal astigmatism. *J Cataract Refract Surg*. 2013;39(12):1803-1809. doi:10.1016/j.jcrs.2013.06.027
7. LaHood BR, Goggin M, Beheregaray S, Andrew NH, Esterman A. Comparing total keratometry measurement on the IOLMaster 700 with Goggin nomogram adjusted anterior keratometry. *J Refract Surg*. 2018;34(8):521-526.
8. LaHood BR, Goggin M, Esterman A. Assessing the likely effect of posterior corneal curvature on toric IOL calculation for IOLs of 2.50 D or greater cylinder power. *J Refract Surg*. 2017;33(11):730-734. doi:10.3928/1081597X-20170829-03
9. Langenbucher A, Hoffmann P, Cayless A, Wendelstein J, Szentmáry N. Evaluation of statistical correction strategies for corneal back surface astigmatism with toric lenses—a vector

analysis. *J Cataract Refract Surg*. 2023;50:385-393. doi:10.1097/j.jcrs.0000000000001370
10. Patel S, Tutchenko L. Spotlight on the corneal back surface astigmatism: a review. *Clin Ophthalmol*. 2021;15:3157-3164. doi:10.2147/OPTH.S284616
11. Alpins N. Astigmatism analysis by the Alpins method. *J Cataract Refract Surg*. 2001;27(1):31-49. doi:10.1016/s0886-3350(00)00798-7
12. Alpins NA, Goggin M. Practical astigmatism analysis for refractive outcomes in cataract and refractive surgery. *Surv Ophthalmol*. 2004;49(1):109-122. doi:10.1016/j.survophthal.2003.10.010
13. Liou HL, Brennan NA. Anatomically accurate, finite model eye for optical modeling. *J Opt Soc Am A Opt Image Sci Vis*. 1997;14(8):1684-1695. doi:10.1364/josaa.14.001684
14. Meng XL, Xiao L, Rubin DB. Maximum likelihood estimation via the ECM algorithm. *Biometrika*. 1993;80(2):267-278. doi:10.1093/biomet/80.2.267
15. Haigis W, Lege B, Miller N, Schneider B. Comparison of immersion ultrasound biometry and partial coherence interferometry for intraocular lens calculation according to Haigis. *Graefes Arch Clin Exp Ophthalmol*. 2000;238(9):765-773. doi:10.1007/s004170000188
16. Langenbucher A, Cayless A, Szentmáry N, Weisensee J, Wendelstein J, Hoffmann P. Prediction of total corneal power from measured anterior corneal power on the IOLMaster 700 using a feedforward shallow neural network. *Acta Ophthalmol*. 2022;100(5):e1080-e1087. doi:10.1111/aos.15040
17. Langenbucher A, Szentmáry N, Cayless A, Weisensee J, Wendelstein J, Hoffmann P. Prediction of corneal back surface power - deep learning algorithm versus multivariate regression. *Ophthalmic Physiol Opt*. 2022;42(1):185-194. doi:10.1111/opo.12909
18. Langenbucher A, Szentmáry N, Cayless A, Wendelstein J, Hoffmann P. Prediction of corneal power vectors after cataract surgery with toric lens implantation—a vector analysis. *PLoS One*. 2023;18(9):e0288316. doi:10.1371/journal.pone.0288316
19. Sexton J, Swensen AR. ECM algorithms that converge at the rate of EM. *Biometrika*. 2000;87(3):651-662. doi:10.1093/biomet/87.3.651
20. Farrell PJ, Salibian-Barrera M, Naczk K. On tests for multivariate normality and associated simulation studies. *J Stat Comput Simul*. 2007;77(12):1065-1080. doi:10.1080/10629360600878449
21. Royston TP. Approximating the Shapiro-Wilk W-test for non-normality. *Stat Comput*. 1992;2:117-119. doi:10.1007/BF01891203
22. Mustafa NH, Ray S. An optimal extension of the centerpoint theorem. *Comput Geom*. 2009;42(6–7):505-510. doi:10.1016/j.comgeo.2007.10.004
23. Welk M, Breuß M. The convex-Hull-stripping median approximates affine curvature motion. In: Lellmann J, Burger M, Modersitzki J, eds. *Scale Space and Variational Methods in Computer Vision. Lecture Notes in Computer Science*. Vol 11603. Springer; 2019:198-210. doi:10.1007/978-3-030-22368-7_16
24. Small CG. A survey of multidimensional medians. *Int Stat Rev*. 1990;58(3):263-277. doi:10.2307/1403809
25. Small CG. Measures of centrality for multivariate and directional distributions. *Canadian J Stat*. 1987;5(1):31-39. doi:10.2307/3314859
26. Asiedu K, Kyei S, Ampiah EE. Autorefraction, retinoscopy, Javal's rule, and Grosvenor's modified Javal's rule: the best predictor of refractive astigmatism. *J Ophthalmol*. 2016;2016:3584137. doi:10.1155/2016/3584137
27. Grosvenor T, Quintero S, Perrigin DM. Predicting refractive astigmatism: a suggested simplification of Javal's rule. *Am J Optom Physiol Optic*. 1988;65(4):292-297.
28. Preussner PR, Hoffmann P, Wahl J. Impact of posterior corneal surface on toric intraocular lens (IOL) calculation. *Curr Eye Res*. 2015;40(8):809-814. doi:10.3109/02713683.2014.959708
29. Wendelstein JA, Hoffmann PC, Hoffer KJ, et al. Differences between keratometry and total keratometry measurements in a large dataset obtained with a modern swept source optical coherence tomography biometer. *Am J Ophthalmol*. 2023;12(260):102-114. doi:10.1016/j.ajo.2023.12.003
30. Lu W, Li Y, Savini G, et al. Comparison of anterior segment measurements obtained using a swept-source optical coherence tomography biometer and a Scheimpflug-Placido tomographer. *J Cataract Refract Surg*. 2019;45(3):298-304. doi:10.1016/j.jcrs.2018.10.033
31. Reitblat O, Levy A, Kleinmann G, Abulafia A, Assia EI. Effect of posterior corneal astigmatism on power calculation and alignment of toric intraocular lenses: comparison of methodologies. *J Cataract Refract Surg*. 2016;42(2):217-225.
32. Savini G, Næser K, Schiano-Lomoriello D, Ducoli P. Optimized keratometry and total corneal astigmatism for toric intraocular lens calculation. *J Cataract Refract Surg*. 2017;43(9):1140-1148.
33. Savini G, Taroni L, Schiano-Lomoriello D, Hoffer KJ. Repeatability of total Keratometry and standard keratometry by the IOLMaster 700 and comparison to total corneal astigmatism by Scheimpflug imaging. *Eye (Lond)*. 2021;35(1):307-315. doi:10.1038/s41433-020-01245-8
34. Tutchenko L, Patel S, Voytsekhivskyy O, Skovron M, Horak O. The impact of changes in corneal back surface astigmatism on the residual astigmatic refractive error following routine uncomplicated phacoemulsification. *J Ophthalmol*. 2020;2020:7395081. doi:10.1155/2020/7395081

How to cite this article: Langenbucher A, Taroni L, Coutinho CP, et al. Evaluating keratometry and corneal astigmatism data from biometers and anterior segment tomographers and mapping to reconstructed corneal astigmatism. *Clin Exp Ophthalmol*. 2024;52(6):627-638. doi:10.1111/ceo.14387